

# Impact of UV radiation from giant spirals on the evolution of dwarf galaxies

S. Mashchenko,<sup>1,2</sup> C. Carignan,<sup>2</sup> and A. Bouchard<sup>2,3</sup>

<sup>1</sup>*Department of Physics and Astronomy, McMaster University, Hamilton, ON, L8S 4M1, Canada*

<sup>2</sup>*Département de physique and Observatoire du mont Mégantic, Université de Montréal, C.P. 6128, Succ. Centre-ville, Montréal, Québec, H3C 3J7, Canada*

<sup>3</sup>*Australia Telescope National Facility, PO Box 76, Epping, NSW 1710, Australia*

23 October 2018

## ABSTRACT

We show that ultraviolet radiation, with wavelengths shorter than 2000 Å, escaping from the disks of giant spirals could be one of the principal factors affecting the evolution of low mass satellite galaxies. We demonstrate, using an analytical approach, that the Lyman continuum part of the radiation field can lead to the ionization of the ISM of dwarf galaxies through the process of photoevaporation, making the ISM virtually unobservable. The FUV part ( $912 < \lambda < 2000$  Å) is shown to dominate over the internal sources of radiation for most of the Galactic dwarf spheroidals. The proposed environmental factor could be at least partially responsible for the bifurcation of the low mass proto-galaxies into two sequences — dwarf irregulars and dwarf spheroidals. We discuss many peculiarities of the Local Group early-type dwarfs which can be accounted for by the impact of the UV radiation from the host spiral galaxy (Milky Way or M31).

**Key words:** galaxies: dwarf – galaxies: evolution – galaxies: ISM – Local Group.

## 1 INTRODUCTION

The diverse group of low luminosity ( $M_V > -12^m5$ ) Local Group dwarf galaxies is loosely divided (based on their recent star formation history, SFH, and neutral gas content) into three categories: dwarf irregulars (dIrr), intermediate type dwarfs (dIrr/dSph), and dwarf spheroidals (dSph). Despite some obvious differences, these galaxies do share a few important properties: (a) they are pressure supported (rotation is dynamically unimportant); (b) for a given luminosity, they have comparable spatial extent (especially when considering the distribution of the old stars); (c) they have comparable low metallicity  $[\text{Fe}/\text{H}] \sim -2$ ; (d) in most cases, they have very aspheric shapes with ellipticity  $e \sim 0.2 - 0.4$ ; (e) the available kinematic data suggest that they are dark matter (DM) dominated.

Local Group dSph galaxies are known to have a wide range of SFHs — from being consistent with a single burst scenario (e.g. Ursa Minor) to the very complex multiple bursts case of Carina (Grebel 1997). Low luminosity dSphs have not formed stars for at least a Gyr. Intermediate type (dIrr/dSph) Local Group dwarfs (LGS 3, Antlia, and Phoenix) had their most recent star bursts  $\sim 100$  Myr ago (Miller et al. 2001; Piersimoni et al. 1999; Martínez-Delgado, Gallart & Aparicio 1999). Intrinsically faint dIrr galaxies are all forming stars at the present time

but with low efficiency ( $dm/dt < 0.001 M_\odot \text{ yr}^{-1}$ , Mateo 1998).

A few scenarios have been proposed to explain the complex SFH of dSph galaxies, including episodic accretion of intergalactic gas (Silk, Wyse & Shields 1987), ISM heating by SN Ia leading to prolonged periods of time with no star formation (Burkert & Ruiz-Lapuente 1997), and bar induced star bursts in the tidally stirred dwarfs scenario of Mayer et al. (2001).

Aside from the differences in the present day star formation rate (SFR), low luminosity galaxies from the sequence dIrr – dIrr/dSph – dSph differ in their neutral gas content. Local Group dIrrs are gas rich: the ratio of the H I mass to the V-band luminosity  $M_{\text{HI}}/L_V$  ranges from  $\sim 1.4$  for GR 8 to  $\sim 2.8$  for DDO 210 (Mateo 1998). Intermediate type dwarfs have smaller H I content: from  $M_{\text{HI}}/L_V \sim 0.14$  for Phoenix (St-Germain et al. 1999; Gallart et al. 2001) to  $M_{\text{HI}}/L_V \sim 0.4$  for LGS 3 (Mateo 1998) and Antlia (Barnes & de Blok 2001). Dwarf spheroidals have no or little H I. The only possible detection with the H I emission located within the optical extent of the dSph and the radial velocity of the gas being within  $15 \text{ km s}^{-1}$  from the optical velocity of the dwarf is that of Sculptor ( $M_{\text{HI}}/L_V \sim 0.09$ , Carignan et al. 1998; Bouchard, Carignan & Mashchenko 2003).

The location of the intrinsically faint Local Group

arXiv:astro-ph/0203317v2 8 Apr 2004

dwarfs on the dSph – dIrr/dSph – dIrr sequence appears to correlate with their proximity to large spirals (e.g. van den Bergh 1999): dSphs are concentrated in the vicinity of the Milky Way and M31, low mass dIrrs are isolated systems, and the intermediate type dwarfs are somewhere in between. Environment appears to bear a significant impact on the dwarfs evolution.

We propose a novel mechanism which can explain the differences in SFHs and neutral gas content between dSphs and dIrrs. Our hypothesis is that the electromagnetic radiation (especially Lyman continuum, LyC, and far ultraviolet, FUV) escaping from the host spiral galaxy can play a decisive role in the evolution of dSphs. Significant amounts of gas can be ionized and heated by the host galaxy LyC when dSphs are on the relatively high galactic latitude parts of their orbits. FUV can also play a role by preventing the formation of the cold neutral medium (CNM) phase of the ISM, which presence is believed to be required for star formation. Moving along their orbits around the host galaxy, dSphs spend relatively short periods of time near the plane of the host, where the fluxes of the LyC and FUV radiation drop to lower metagalactic levels. For some of the dwarfs, the time spent in the shadow produced by the H I disk of the host spiral is enough for their ISM to recombine, cool down and form stars in a short burst. The timescale for the repeated star bursts in this scenario is equal to half of the orbital period, or  $\sim 1-5$  Gyr, which is in agreement with the observed SFHs. dSph galaxies with total masses  $< 2 \times 10^8 M_{\odot}$  gradually lose their ISM when the gas is ionized and heated to  $\sim 10^4$  K by the LyC radiation from the host galaxy, leading to the globally declining SFR. This should affect more the dwarfs on almost polar orbits, because their ISM is being kept ionized for the largest fraction of their lifetimes.

This paper is organized as follows. Section 2 presents our analytical model of the photoionization of the ISM of dSphs by the LyC radiation from the host spiral galaxy, and evaluates the importance of the external FUV radiation for Galactic dSphs. Section 3 gives the observational evidence for the impact of the electromagnetic radiation from giant spirals on the evolution of dwarf satellite galaxies. Section 4 discusses the implications of our results and gives our conclusions.

## 2 MODEL

### 2.1 LyC radiation: a toy model

We adopt the following very simple description of the Galactic ionizing radiation field. Total LyC luminosity of the Galaxy is  $L_0 = 3 \times 10^{53} \text{ s}^{-1}$ . The escape fraction of LyC photons is  $f_{\text{esc}} = 0.1$  in all directions except for a narrow zone of  $\pm 15^\circ$  near the Galactic plane where it is equal to zero. The background LyC flux is  $F_{\text{bg}} = 10^4 \text{ cm}^{-2} \text{ s}^{-1}$ . In this model the angle-averaged value of the escape fraction is  $\langle f_{\text{esc}} \rangle \simeq 0.07$ , which is consistent with the observational upper limits on the metagalactic ionizing background (Shull et al. 1999; Bianchi, Cristiani & Kim 2001). The derived radius of the sphere centred on the Milky Way where the Galactic ionizing flux dominates the metagalactic flux is 224 kpc.

First we consider the following toy model for the ISM of

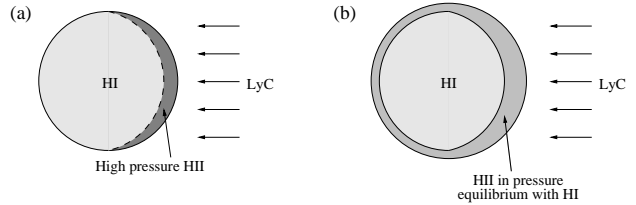


**Figure 1.** Photoevaporation of the ISM of a dSph galaxy exposed to the LyC photons escaping from the disk of the host galaxy: (a) on the side facing the source of the ionizing radiation a thin layer of the high pressure photoionized hydrogen is formed; (b) trying to reach a pressure equilibrium with the neutral gas, the H II gas expands and fills the outer regions of the galaxy, allowing a fresh layer of H I to be ionized. The process repeats itself until the H I gas is fully ionized, or until the ionized gas on the irradiated side of the cloud becomes optically thick to the LyC photons.

a dSph: a homogeneous isothermal H I sphere with the initial radius  $R_0 = 500$  pc, temperature  $T_0 = (5-10) \times 10^3$  K, and number density  $n_0 = 0.01 \text{ cm}^{-3}$ . The gas pressure is  $P_0/k = 50-100 \text{ K cm}^{-3}$ . The temperatures of  $(5-10) \times 10^3$  K are typical for a warm neutral medium (WNM) phase of the ISM (Wolfire et al. 1995). The mass of the gas is  $M_{\text{HI}} = 1.3 \times 10^5 M_{\odot}$ . The H I column density through the centre of the cloud is  $N_0 = 3.1 \times 10^{19} \text{ cm}^{-2}$ .

For Galactic satellites with measured proper motions (LMC, Sculptor, Ursa Minor, and Fornax), the radial component of the space velocity in the Galactic frame of reference is much smaller than the tangential component (Schweitzer, Cudworth & Majewski 1997; Piatek et al. 2002), suggesting low eccentricity orbits. Integration of orbits of the satellites in the Galactic isothermal halo potential gives a small ratio of apocentric to pericentric distances  $R_a/R_p \simeq 2-2.4$  (Johnston 1998). For simplicity, for the rest of the paper we will assume that the orbits of the Galactic satellites have zero eccentricity.

We place our toy dSph on a circular orbit around the Milky Way at a distance of  $R = 100$  kpc, which is the distance of Carina — the dwarf spheroidal with probably the most puzzling star formation history consisting of three star bursts separated by 4-8 Gyr (Hurley-Keller, Mateo & Nemeč 1998). In our model, the Galactic ionizing flux at such a distance is  $2.5 \times 10^4 \text{ cm}^{-2} \text{ s}^{-1}$ . When we include the background radiation, the total LyC flux rises to  $F_{\text{tot}} = 3.5 \times 10^4 \text{ cm}^{-2} \text{ s}^{-1}$ .

Can such a low LyC flux photoionize H I in our toy model? The answer appears to be “no” as the flux of LyC photons  $F_{\text{tot}}$  is less than the recombination rate  $F_0$  along a line crossing the centre of the cloud:  $F_0 = 2R_0 n_0^2 \alpha_0^{(2)} = 8 \times 10^4 \text{ cm}^{-2} \text{ s}^{-1}$ . (Here  $\alpha_0^{(2)} \simeq 2.6 \times 10^{-13} \text{ cm}^3 \text{ s}^{-1}$  at  $10^4$  K is the coefficient of recombination to all but the ground level of the hydrogen atom.)

An important caveat is that in an H I cloud exposed to anisotropic ionizing radiation field the gas which is being photoionized does not stay at its original location. The increased pressure pushes the photoionized gas away, exposing new H I to the incident LyC radiation. This process termed photoevaporation has been studied both analytically (Bertoldi 1989; Bertoldi & McKee 1990) and numerically (Lefloch & Lazareff 1994) in application to an interstellar cloud exposed to the ionizing flux from a nearby hot star.

This theory is not directly applicable to the case of the ISM of a dSph galaxy because of the invalidity of the following assumptions adopted by the authors: 1) the temperature of the neutral gas is much lower than the temperature of the ionized gas  $T_{\text{HII}} \simeq 10^4$  K; 2) initially the cloud is in pressure equilibrium with the intercloud medium; 3) the ionized gas is not gravitationally bound to the cloud, and can freely flow away.

Nevertheless, we argue that the process of photoevaporation can also take place in the ISM of a dwarf galaxy. Even in the case of the highest possible WNM temperature  $T_{\text{HI}} \simeq 10^4$  K, the pressure of the photoionized gas is  $\sim 2$  times higher than the original pressure of H I (because during the photoionization of hydrogen the number of particles doubles, and the temperature is maintained at the  $T_{\text{HII}} \simeq 10^4$  K level when the heating by the LyC photons is balanced by radiative cooling). Unlike the interstellar cloud case, in photoevaporating ISM of a reasonably massive dwarf galaxy the ionized gas can stay gravitationally bound to the galaxy. Higher pressure causes the H II gas to expand, filling the outer regions of the galaxy, allowing a fresh layer of H I to be ionized (Fig. 1). The speed with which the ionization front propagates inside the cloud is determined by how fast the photoionized gas can flow away and be redistributed in the outer parts of the dwarf galaxy, and is expected to be less than or comparable to the isothermal sound speed in the H II region  $c_g = 11.7 \text{ km s}^{-1}$ .

Under the assumption that during photoionization the H II gas reaches a state of pressure equilibrium with the H I gas (so the final pressure  $P_1$  is equal to the initial pressure  $P_0$ ), the parameters for the fully photoionized cloud are  $R_1 = \chi^{1/3} R_0$ ,  $n_1 = \chi^{-1} n_0$ ,  $N_1 = \chi^{-2/3} N_0$ , and  $F_1 = \chi^{-5/3} F_0$ . (Here  $\chi \equiv 2T_1/T_0$ .) Assuming the H II temperature of  $T_1 = 10^4$  K, we obtain  $\chi = 2 - 4$ , so the final radius  $R_1$ , number density  $n_1$ , column density  $N_1$  and minimum LyC flux  $F_1$  required to keep the cloud fully ionized are  $R_1 = 630 - 790$  pc,  $n_1 = (2.5 - 5) \times 10^{-3} \text{ cm}^{-3}$ ,  $N_1 = (1.2 - 1.9) \times 10^{19} \text{ cm}^{-2}$ , and  $F_1 = (0.8 - 2.5) \times 10^4 \text{ cm}^{-2} \text{ s}^{-1}$ . The photoevaporation time scale is of the order of  $2R_0/c_g = 84$  Myr. Once the dwarf moves in the shadow produced by the Galactic H I layer, the gas will recombine with a time scale of  $\tau_{\text{rec}} = 1/(\alpha_0^{(2)} n_1) = 24 - 49$  Myr. Both photoevaporation and recombination time scales are a small fraction of the dSph's orbital periods of a few Gyr.

Assuming that the process of photoevaporation is 100% efficient, in our toy model the ISM of a dwarf located  $\sim 100$  kpc away from the Milky Way can be fully photoionized by the Galactic LyC photons:  $F_1 < F_{\text{tot}}$ . Once the dwarf moves into the shadow produced by the Galactic disk, the gas can recombine on a relatively short time scale, potentially leading to an episode of star formation.

## 2.2 LyC radiation: more realistic approach

A homogeneous gas sphere is admittedly not a very realistic model for the ISM of dSphs. In our next step we consider the distribution of isothermal ionized hydrogen gas being in hydrostatic equilibrium inside properly normalized DM halos with different masses and density profiles (either NFW, or Burkert 1995). The temperature of the gas is  $T_1 = 10^4$  K, so the sound speed is  $c_g = 11.7 \text{ km s}^{-1}$ . Similarly to the toy model, we wish to find the lowest ionizing flux  $F_1$  suffi-

cient to keep the ISM fully photoionized by estimating the recombination rate along a line crossing the centre of the cloud.

The analytical formulae describing the hydrostatic equilibrium distribution of isothermal gas inside NFW and Burkert's DM halos were derived by Sternberg, McKee & Wolfire (2002, Appendix A). For NFW halos, these authors give the following expressions for the dimensionless DM density  $f_\rho$ , enclosed DM mass  $f_M$ , and gas density  $f_{\text{gas}}$ :

$$f_\rho = 1/[x(1+x)^2], \quad (1)$$

$$f_M = 3[\ln(1+x) - x/(1+x)], \quad (2)$$

$$f_{\text{gas}} = e^{-3(v_s/c_g)^2} (1+x)^{(v_s/c_g)^2/x}. \quad (3)$$

Here  $x \equiv r/r_s$  is the dimensionless radius. The corresponding equations for Burkert's halos are

$$f_\rho = 1/[(1+x)(1+x^2)], \quad (4)$$

$$f_M = (3/2)\{[\ln(1+x^2)]/2 + \ln(1+x) - \tan^{-1} x\}, \quad (5)$$

$$f_{\text{gas}} = [e^{-(1+1/x)\tan^{-1} x} \times (1+x)^{(1+1/x)}(1+x^2)^{(1/x-1)/2}]^{(3/2)(v_s/c_g)^2}. \quad (6)$$

From equations (16), (17) and (19) of Sternberg et al. (2002) we obtained the following approximate expressions for the scaling radius  $r_s$ , the scaling velocity  $v_s$ , and the concentration parameter  $x_{\text{vir}} \equiv r_{\text{vir}}/r_s$  for DM halos in  $\Lambda$ CDM cosmology (assuming  $\Omega_m = 0.3$ ,  $\Omega_\Lambda = 0.7$ ,  $H_0 = 70 \text{ km s}^{-1} \text{ Mpc}^{-1}$ , and  $\sigma_8 = 1$ ):

$$r_s = 0.96 \left( \frac{m_{\text{vir}}}{10^9 M_\odot} \right)^{0.41} \text{ kpc}, \quad (7)$$

$$v_s = 24.7 \left( \frac{m_{\text{vir}}}{10^9 M_\odot} \right)^{0.31} \text{ km s}^{-1}, \quad (8)$$

$$x_{\text{vir}} = 26.2 \left( \frac{m_{\text{vir}}}{10^9 M_\odot} \right)^{-0.07}. \quad (9)$$

Here  $r_{\text{vir}}$  and  $m_{\text{vir}}$  are the virial radius and the virial mass of a dwarf, respectively. Equations (7-9) are valid for  $m_{\text{vir}} = 10^8 - 10^{11} M_\odot$ .

The total masses of the Galactic dwarf spheroidals are not known. Even under the simplest ‘‘mass follows light’’ assumption, most dSphs appear to be DM dominated (Mateo 1998). The absence of tidal features caused by the gravitational field of the Milky Way in stellar isophots of Draco down to a very low level (0.001 of the central surface brightness) suggests that at least in this dSph the DM halo is more extended than the stellar body (Odenkirchen et al. 2001). Comparison of the structure and kinematics of Milky Way satellites with cosmological N-body  $\Lambda$ CDM simulations suggests that the dSphs may represent the most massive substructures in the Galactic DM halo, with masses up to a few  $10^9 M_\odot$  (Stoehr et al. 2002; Hayashi et al. 2003). By allowing stars and DM to have different velocity distributions, Lokas' (2002) analysis of the observed radial profiles of stellar velocity dispersion for Fornax and Draco yielded a range of possible total masses of  $\sim (1 - 4) \times 10^9 M_\odot$  for each of these dwarfs. (The analysis included both NFW-type and flat-core-type DM profiles.)

In this paper we explore the range of virial masses of dwarf spheroidals between  $2.5 \times 10^8$  and  $4 \times 10^9 M_\odot$ , with a fiducial value of  $10^9 M_\odot$ . Galaxies less massive than  $\sim 2 \times 10^8 M_\odot$  will not be able to keep the photoionized gas gravitationally bound for a long period of time (unless they are confined by non-negligible pressure of the hot Galactic corona), and more massive than a few  $10^9 M_\odot$  will be inconsistent with the predictions of  $\Lambda$ CDM models.

The halos of the dSphs are truncated by the Galactic tidal field. We estimate the tidal radius  $r_t$  of satellites by solving numerically the following non-linear equation applicable to dwarfs on circular orbits around the host (Hayashi et al. 2003):

$$\frac{m(r_t)}{r_t^3} = \frac{M(R)}{R^3} \left[ 2 - \frac{R}{M(R)} \frac{\partial M}{\partial R} \right]. \quad (10)$$

Here  $m(r) = f_M(r/r_s)v_s^2 r_s/G$  and  $M(R)$  are the enclosed DM mass for the satellite and host, and  $R$  is the distance of the satellite from the centre of the host. We assume that the Milky Way DM halo is an isothermal sphere, with  $M(R) = 2\sigma^2 R/G$ . We set  $\sigma = 113.6 \text{ km s}^{-1}$  so that  $M(250 \text{ kpc}) = 1.5 \times 10^{12} M_\odot$ . For the range of galactocentric distances of dSphs ( $R = 70 - 250 \text{ kpc}$ ), the mass of a tidally truncated satellite  $m_t$  is found to be more than half of the original virial mass  $m_{\text{vir}}$ .

Our algorithm is as follows. For a given satellite's halo model (Burkert or NFW), virial mass  $m_{\text{vir}}$ , and galactocentric distance  $R$ , we first find the tidal radius  $r_t$  by solving the non-linear equation (10). The recombination rate  $F_1$  along a line crossing the centre of the halo is given by

$$F_1 = 2\alpha_0^{(2)} n_0^2 r_s \int_0^{x_t} f_{\text{gas}}^2(x) dx. \quad (11)$$

Here  $x_t \equiv r_t/r_s$  is the dimensionless tidal radius and  $n_0$  is the central proton number density of the gas.

Substituting  $F_1$  in equation (11) with the total LyC flux at the distance  $R$  from the Galactic centre  $F_{\text{tot}} = F_{\text{bg}} + f_{\text{esc}} L_0 / (4\pi R^2)$  and solving the resulting equation for  $n_0$  gives us an estimate of the largest possible central number density  $n_{0,\text{tot}}$  for the ISM being in a fully photoionized state when the satellite is located high above the Galactic plane:

$$n_{0,\text{tot}} = \left[ \frac{F_{\text{bg}} + f_{\text{esc}} L_0 / (4\pi R^2)}{2\alpha_0^{(2)} r_s \int_0^{x_t} f_{\text{gas}}^2(x) dx} \right]^{\frac{1}{2}}. \quad (12)$$

Similarly, substituting  $F_1$  with  $F_{\text{bg}}$  will result in the estimate of the largest possible central number density  $n_{0,\text{bg}}$  for the ISM being in a fully photoionized state when the dwarf is located near the Galactic plane (in the shadow produced by the H I disk of the Milky Way):

$$n_{0,\text{bg}} = \left[ \frac{F_{\text{bg}}}{2\alpha_0^{(2)} r_s \int_0^{x_t} f_{\text{gas}}^2(x) dx} \right]^{\frac{1}{2}}. \quad (13)$$

The corresponding maximum total masses  $m_{\text{gas,tot}}$  and  $m_{\text{gas,bg}}$  of the fully photoionized ISM are

$$m_{\text{gas,tot/bg}} = 4\pi n_{0,\text{tot/bg}} m_{\text{HI}} r_s^3 \int_0^{x_t} f_{\text{gas}}(x) x^2 dx. \quad (14)$$

Here  $m_{\text{HI}}$  is the mass of a hydrogen atom. From equations (12-14) one can see that the following inequalities hold for any finite  $R$ :  $n_{0,\text{tot}} > n_{0,\text{bg}}$  and  $m_{\text{gas,tot}} > m_{\text{gas,bg}}$ .

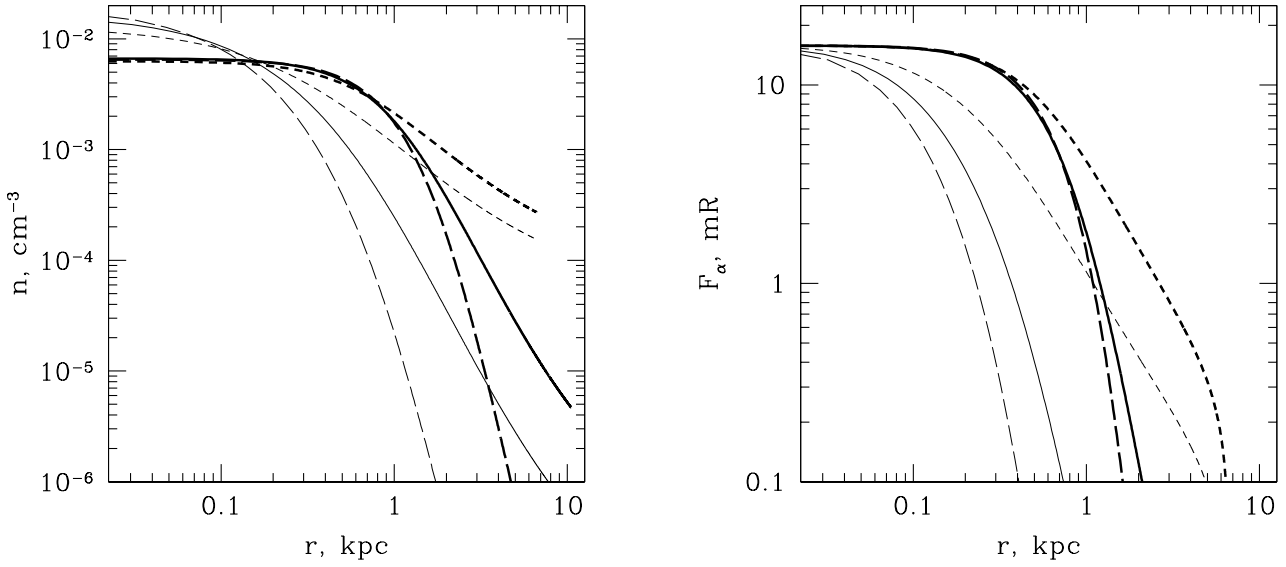
In Fig. 2 we show the critical gas density profiles for different halos located at a distance of 100 kpc from the Milky Way (left panel). By ‘‘critical’’ we mean the ISM for which the recombination rate along a line crossing the centre of the dwarf is equal to the incident LyC flux. The central number density and mass for such an ISM are described by equations (12-14). Subcritical (with lower  $n_0$ ) and critical ISM are fully photoionized, whereas a supercritical (with higher  $n_0$ ) ISM has a neutral core where star formation can take place. (The  $H_\alpha$  surface brightness profiles for our model halos shown in the right panel of Fig. 2 will be discussed at the end of this section.)

As can be seen in Fig. 2, in the lowest mass cases ( $m_{\text{vir}} = 2.5 \times 10^8 M_\odot$ ) the photoionized gas is not well confined by the gravity of the satellite, with the gas density at the tidal radius being only 20 – 80 times lower than the central density. On the other hand, the gas pressure at the tidal radius is low — around  $4 \text{ K cm}^{-3}$ , so even very tenuous Galactic corona with temperature of  $10^6 \text{ K}$  and proton number density of  $2 \times 10^{-6} \text{ cm}^{-3}$  would suffice to confine the gas.

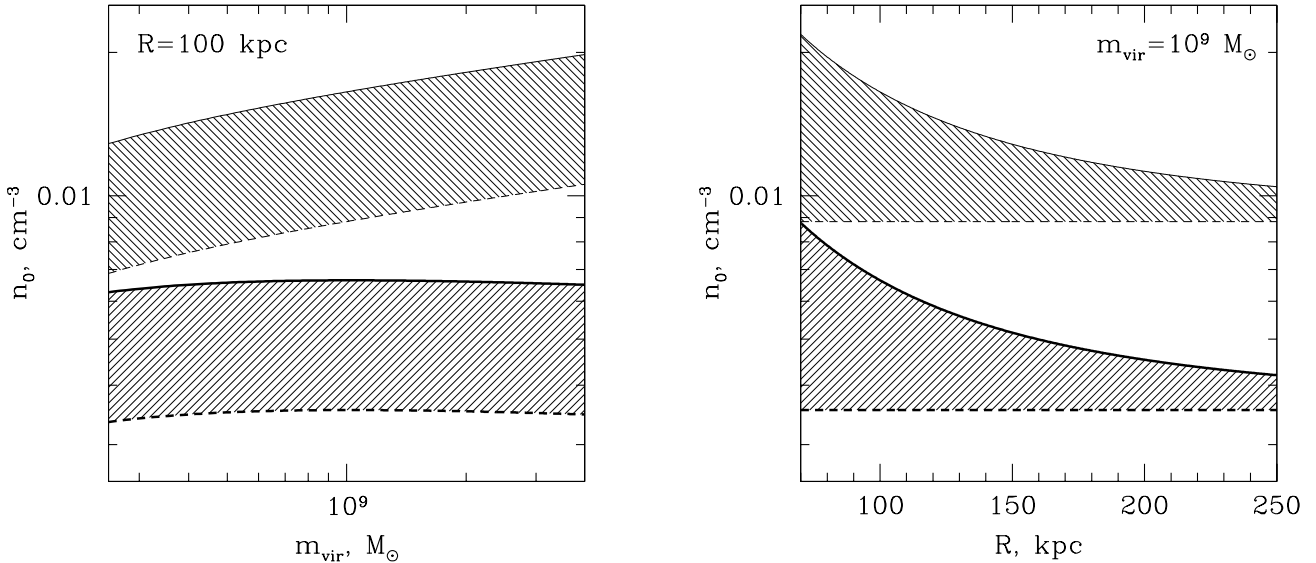
In Fig. 2 one can also see that the isothermal gas density distribution for Burkert halos has a large core with an almost constant radius of  $\sim 800 \text{ pc}$  for the whole range of virial masses considered. On the other hand, the ISM in NFW halos is more centrally peaked, which is the result of their cuspy DM density profile.

Fig. 3 shows critical central gas density for either Burkert or NFW halos with different virial masses, located at different distances from the Milky Way, and exposed either to the total (Galactic + metagalactic) ionizing flux, or only to the background LyC radiation (when the halo is in the shadow produced by the Galactic disk). The shaded areas correspond to halos which are subcritical when they are exposed to the Milky Way ionizing radiation, and supercritical when they are in the ‘‘LyC shadow’’ and can potentially form stars. These *half-critical* systems are of utmost interest to us as they can explain both the multiple star bursts history of some of the Galactic dSphs and the apparent absence of ISM in all of them (with the possible exception of Sculptor, Boucard et al. 2003) including such dwarfs as Carina and Fornax which have had some star formation in the last Gyr.

By analyzing Fig. 3 we can make a few interesting observations. First, the range of central densities for half-critical dwarfs is almost independent on the virial mass of the halo, especially for Burkert halos. Second, this range is relatively large (a factor of 2 or more) for dwarfs located  $\lesssim 100 \text{ kpc}$  from the Galaxy, but quickly becomes much smaller for larger distances. At the distance of Leo I (250 kpc), the interval is so narrow, that it would be very unlikely if the ISM of this galaxy was in the half-critical state. If the dwarf has any ISM, the gas is probably thin enough to be photoionized by the metagalactic LyC background alone. In the past it could have possessed a denser ISM with a neutral core where star formation could have taken place.



**Figure 2.** Radial profiles for critical ISM in Burkert (thick lines) and NFW (thin lines) halos with virial masses of  $10^9 M_{\odot}$  (solid lines),  $2.5 \times 10^8 M_{\odot}$  (short-dashed lines), and  $4 \times 10^9 M_{\odot}$  (long-dashed lines), located 100 kpc from the Galactic centre high above the plane. Left panel: proton number density. Right panel:  $H_{\alpha}$  surface brightness.



**Figure 3.** Critical central number density for Burkert (thick lines) and NFW (thin lines) halos as a function of the virial mass (left panel) and galactocentric distance (right panel). Both  $n_{0,\text{tot}}$  (solid lines) and  $n_{0,\text{bg}}$  (dashed lines) are shown. The shaded areas show the locus of half-critical halos.

Critical total gas masses for different halos are shown in Fig. 4. Burkert halos can contain much more massive ISM in half-critical (shaded areas) or permanently photoionized (areas below the dashed lines) states than NFW halos because they are less centrally concentrated. The total mass of gas in half-critical halos is of order of  $10^6 M_{\odot}$  (Burkert) or  $10^5 M_{\odot}$  (NFW). As the right panel of Fig. 4 suggests, isolated Burkert halos can contain millions  $M_{\odot}$  of gas within their virial radii kept fully photoionized by the metagalactic ionizing radiation alone.

Only a fraction of the total mass of gas in a half-critical halo can recombine, cool down and collapse toward the centre of the dwarf to be available for star formation during a relatively short passage of the satellite through the “LyC shadow” cast by the Galactic disk. In our isothermal sphere model for the Milky Way halo, a dwarf on a circular polar orbit with  $R = 100$  kpc will spend 320 Myr in the shadow with the opening angle of  $30^{\circ}$  twice per orbital period (which is equal to 3.8 Gyr).

The shortest recombination, cooling and free-fall time

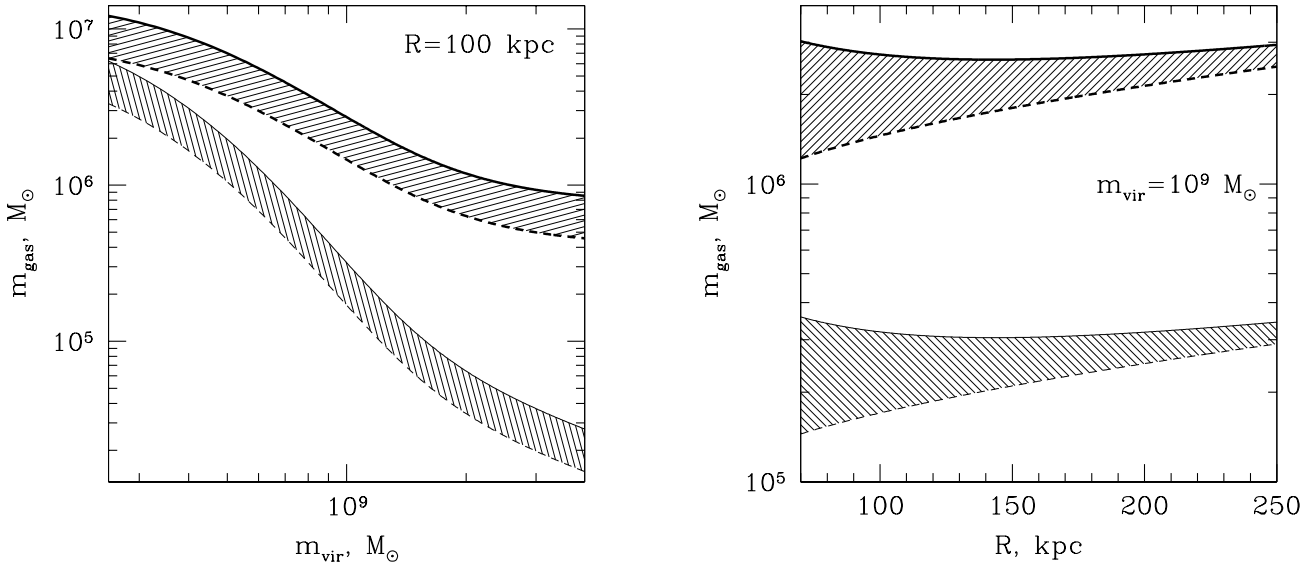


**Figure 4.** Critical total gas mass for Burkert (thick lines) and NFW (thin lines) halos as a function of the virial mass (left panel) and galactocentric distance (right panel). Both  $m_{\text{gas,tot}}$  (solid lines) and  $m_{\text{gas,bg}}$  (dashed lines) are shown. The shaded areas show the locus of half-critical halos.

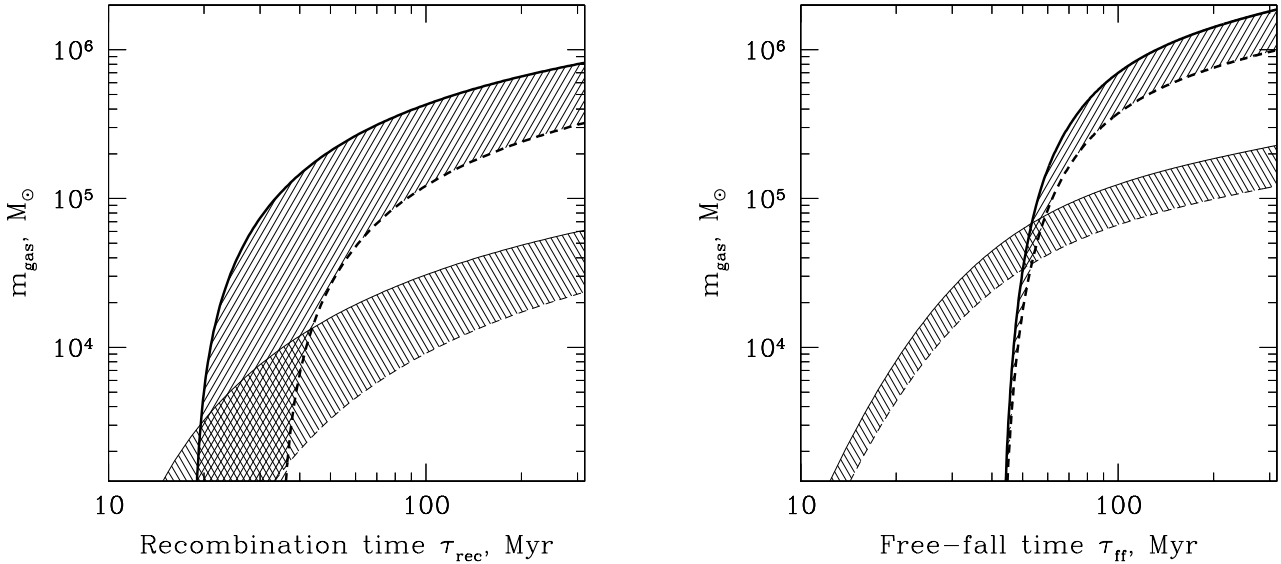


**Figure 5.** Mass of gas for the critical ISM in a Burkert (thick lines) or NFW (thin lines) halo ( $m_{\text{vir}} = 10^9 M_{\odot}$ ,  $R = 100$  kpc) which can recombine (left panel) or collapse (right panel) within the time scale  $\tau$  after the source of the ionizing radiation is turned off. The shaded areas show the locus of half-critical halos.

scales are at the centre of the halo. As time goes on, gas can recombine and collapse at increasingly larger distances from the centre of the halo. Fig. 5 quantifies this effect for a specific case of either a Burkert or a NFW halo with a virial mass of  $10^9 M_{\odot}$  located 100 kpc away from the Galaxy. In this figure we show the recombination time  $\tau_{\text{rec}} = 1/(\alpha_0^{(2)}n)$  and the free-fall time  $\tau_{\text{ff}} = \sqrt{3\pi/(32G\rho)}$  (Binney & Tremaine 1994, p. 184). (Here  $\rho$  is the average total density of the system.) In our notation, the free-fall

time can be written as a function of the dimensionless radius  $x$  in the following way:

$$\tau_{\text{ff}} = \frac{\pi r_s}{v_s} \left[ \frac{x^3}{8f_M(x)} \right]^{\frac{1}{2}}. \quad (15)$$

As can be seen in Fig. 5, the recombination time scale is more important than the free-fall time in controlling how much gas can become available for star formation at the centre of the dwarf. It is also probably more important than

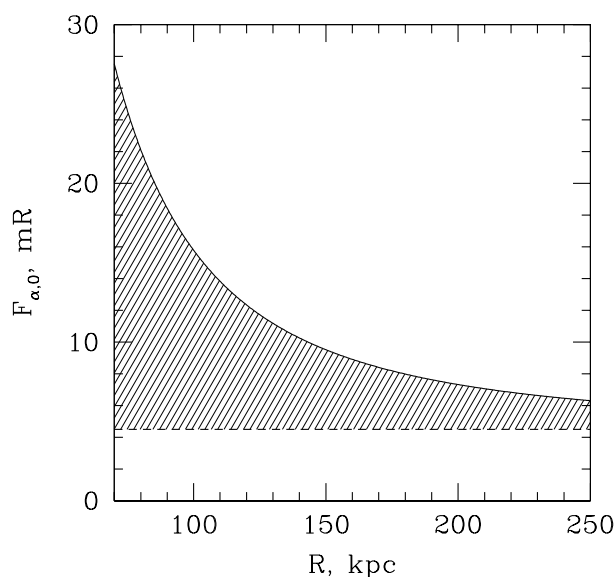


**Figure 6.** Range of possible central  $H_\alpha$  brightness for half-critical halos located at different distances from the Milky Way (the shaded area).

the cooling time  $\tau_{\text{cool}}$  (not shown in Fig. 5). Indeed, both recombination and cooling time scales have the same dependence on density —  $\tau_{\text{rec}} = 0.122/n$  Myr, and  $\tau_{\text{cool}} = 1.31 \times 10^{-25}/(\Lambda n)$  Myr, so only for  $\Lambda < 1.1 \times 10^{-24}$  erg cm<sup>3</sup> s<sup>-1</sup> can cooling become more important than recombination. (Sutherland & Dopita (1993) give the following value for the cooling function of  $10^4$  K gas:  $\Lambda = 4 \times 10^{-24}$  erg cm<sup>3</sup> s<sup>-1</sup>.) In reality, processes of recombination, cooling and collapse of the gas are not independent from each other, and for accurate estimates of how much of cold gas can accumulate at the centre of the halo one has to integrate a system of appropriate differential equations, which is beyond the scope of this paper.

From Fig. 5 one can estimate that in a half-critical halo with  $m_{\text{vir}} = 10^9 M_\odot$  and  $R = 100$  kpc approximately  $5 \times 10^5 M_\odot$  (Burkert profile) or  $5 \times 10^4 M_\odot$  (NFW profile) of gas can collapse to form a denser neutral core during the time spent in the shadow ( $\sim 300$  Myr). It remains to be seen if this time interval is long enough for the formation of molecular hydrogen clouds and eventually stars. The above mass estimates should be considered as upper limits, as the low density gas in the outer parts of the dwarf will remain photoionized by the metagalactic LyC radiation.

The last issue we consider in this section is related to the observability of the photoionized ISM in our model halos in the  $H_\alpha$  spectral line. The  $H_\alpha$  brightness  $F_\alpha$  along a line crossing the halo is related to the corresponding recombination rate of hydrogen  $F_1$  through  $F_\alpha = F_1 \alpha_{32}/\alpha_0^{(2)} \simeq 0.45 F_1$ . Here  $\alpha_{32} = 1.17 \times 10^{-13}$  cm<sup>3</sup> s<sup>-1</sup> (for  $T = 10^4$  K) is the corresponding photon production coefficient (Spitzer 1978, p. 89).

The first observational deep upper limits on the intensity of the  $H_\alpha$  emission from dwarf spheroidals set by Gallagher et al. (2003) for Draco and Ursa Minor are 24 mR and 21 mR, respectively ( $1 \text{ mR} \equiv 10^3 \text{ cm}^{-2} \text{ s}^{-1}$ ). These results were obtained with WHAM (Wisconsin H-Alpha Map-

per) which has an effective beam size of  $1^\circ$ . Do these upper limits exclude the possibility of the presence of half-critical ISM in Draco and Ursa Minor?

Fig. 6 shows the range of central  $H_\alpha$  brightness  $F_{\alpha,0}$  for half-critical halos as a function of the galactocentric distance  $R$  (the shaded area). As one can see, the expected central  $H_\alpha$  flux from Galactic dSphs is very low, with values in the range of 5 – 30 mR and 5 – 21 mR for the distances of Ursa Minor ( $R = 66$  kpc) and Draco ( $R = 82$  kpc), respectively.

These values of  $F_{\alpha,0}$  should not be directly compared with the observations, as the large beam size of WHAM leads to the averaging of  $H_\alpha$  flux over a significant area, effectively reducing the observed surface brightness. This is evident from the right panel of Fig. 2 which shows the radial profile of  $F_\alpha$  for different halos. The effect should be strongest for NFW halos, as their  $H_\alpha$  flux drops significantly on scales of 200 – 300 pc ( $\sim 10'$  at a distance of 100 kpc).

To allow a direct comparison of the WHAM observations with our model, in Fig. 7 we plot the expected  $H_\alpha$  flux  $\langle F_\alpha \rangle$  from half-critical ISM of dSphs averaged over a circular beam with a diameter of  $1^\circ$  centred on the dwarf. Fig. 7 shows that the flux is very low, with NFW halos being  $\sim 10$  times fainter than Burkert’s halos. For both NFW and Burkert halos with masses  $2.5 \times 10^8 - 4 \times 10^9 M_\odot$ , the range of  $\langle F_\alpha \rangle$  for half-critical ISM is 1.3 – 20.7 mR for Ursa Minor and 0.6 – 12.7 mR for Draco. As one can see, the whole range of  $H_\alpha$  brightness expected from half-critical ISM in Galactic dSphs is below the best available observational upper limits.

Finally, in Fig. 8 we show the apparent extent of the  $H_\alpha$  emission for our model halos. Here we plot the angular distance  $r_{\text{gas}}$  from the centre of the dwarf where the  $H_\alpha$  surface brightness drops by a factor of  $e$ . For our range of  $m_{\text{vir}}$  and  $R$ , the angular scalelength of  $H_\alpha$  emission ranges between  $1.5'$  (NFW halo with  $m_{\text{vir}} = 4 \times 10^9 M_\odot$  and  $R = 250$  kpc) and  $37'$  (Burkert halo with  $m_{\text{vir}} = 2.5 \times 10^8 M_\odot$  and  $R = 70$  kpc).

The conclusion we draw here is that to rule out the presence of fully photoionized ISM in half-critical state in Galactic dwarf spheroidals, either much higher sensitivity (down to 0.1 – 0.2 mR) low angular resolution ( $\sim 1^\circ$ ), or lower sensitivity ( $\sim 5$  mR) but much higher angular resolution ( $\sim 1'$ )  $H_\alpha$  observations are required.

### 2.3 FUV radiation

FUV radiation between 912 and 2000 Å, absorbed by interstellar dust, is the most important source of heating for the Galactic neutral ISM (Wolfire et al. 1995). The UV heating is proportional to the density of the gas. The denser CNM phase of the ISM is thus more sensitive to changes in the level of the FUV radiation than the WNM phase, and for sufficiently large FUV fluxes can be completely evaporated (CNM → WNM phase transition). The presence of CNM is believed to be essential for molecular hydrogen cloud formation, and hence for star formation.

Even the smallest isolated dIrr galaxies are known to possess two-phase ISM (Young & Lo 1996, 1997b). Theoretical models predict that a very low level radiation field, 0.001–0.01 of the local Galactic value, produced by stars in a low mass dIrr can maintain its ISM in a two-phase state at pressures  $\sim 10 - 200 \text{ K cm}^{-3}$  (Young & Lo 1997b, their fig. 16). If such a dwarf is exposed to external FUV radiation

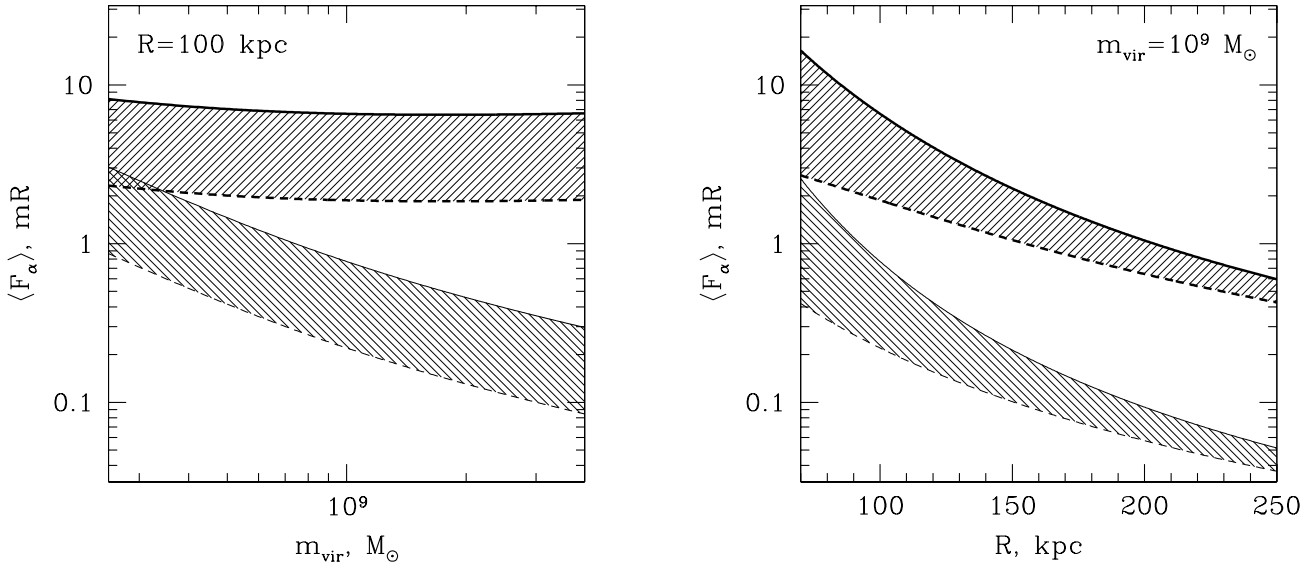


**Figure 7.**  $H_\alpha$  central surface brightness averaged over a  $1^\circ$  circular beam for critical ISM in Burkert (thick lines) and NFW (thin lines) halos as a function of the virial mass (left panel) and galactocentric distance (right panel). Solid (dashed) lines correspond to the external LyC flux  $F_{\text{tot}}$  ( $F_{\text{bg}}$ ). The shaded areas show the locus of half-critical halos.

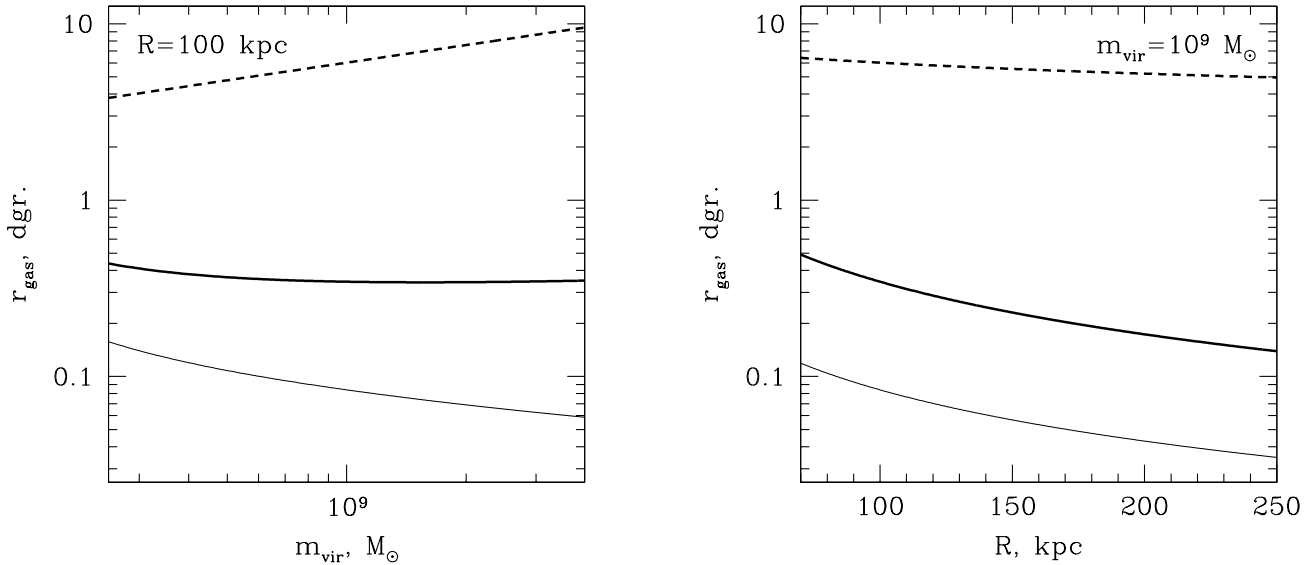


**Figure 8.** Exponential scalelength in angular units of  $H_\alpha$  surface brightness for fully photoionized ISM in Burkert (thick lines) and NFW (thin lines) halos as a function of the virial mass (left panel) and galactocentric distance (right panel). Dashed lines show the apparent tidal radius of DM halos.

(e.g. from a nearby spiral galaxy) with the flux larger than the internal one, the balance between CNM/WNM phases of the ISM will be shifted toward the WNM phase, reducing the SFR. For large enough external FUV flux the star formation will be quenched. Thus it appears that the FUV radiation from giant spirals could be another important environmental factor for intrinsically faint satellite galaxies.

We consider the two following main components of the FUV radiation field inside early-type dwarfs: internal (from

the Population II stars), and external (from the host spiral galaxy).

From table 4 of Welch, Mitchell & Yi (1996) we derive the following estimate of the intensity of the FUV interstellar radiation from the old population stars averaged over the wavelength interval  $900 - 1100 \text{ \AA}$  at the centre of the dwarf elliptical galaxy NGC 185:  $\sim 2000 \text{ cm}^{-2} \text{ s}^{-1} \text{ \AA}^{-1}$ . We assume that the FUV flux at the centre of a dwarf scales as in a homogeneous stellar sphere as  $I_0^{2/3} L_V^{1/3}$ , where



$I_0$  is the central V-band luminosity density and  $L_V$  is the V-band luminosity of the galaxy. For NGC 185, Mateo (1998) gives the following values:  $I_0 = 1.76 L_\odot \text{ pc}^{-3}$  and  $L_V = 1.25 \times 10^8 L_\odot$ . We obtain the following estimate of the FUV flux at the centre of early-type dwarfs, expressed in units of the standard local FUV background with the flux  $F_{loc} = 1.0 \times 10^5 \text{ cm}^{-2} \text{ s}^{-1} \text{ \AA}^{-1}$  at  $\lambda = 1000 \text{ \AA}$  (Draine 1978, their equation [11]):

$$f_{int} \simeq 2.7 \times 10^{-5} I_0^{2/3} L_V^{1/3}, \quad (16)$$

where  $I_0$  is in  $L_\odot \text{ pc}^{-3}$ , and  $L_V$  is in  $L_\odot$ .

The FUV luminosity of the Local Group giant spirals (Milky Way and M31) is not well known. We assume that, for face-on giant spiral galaxies, the FUV flux is proportional to the  $H_\alpha$  flux (because most of both types of radiation can be traced back to the same source — young massive stars). Two nearby face-on spiral galaxies, similar to M31 and the Milky Way in their Hubble type and luminosity, have been observed with the Ultraviolet Imaging Telescope (UIT, Stecher et al. 1997) aboard the space shuttles: NGC 628 (M74) and NGC 5457 (M101). Bell & Kennicutt (2001) presented for these galaxies both FUV flux at  $\lambda = 1521 \text{ \AA}$  (UIT filter B1), and  $H_\alpha$  flux. In accord with our expectations, the ratio of the  $H_\alpha$  flux to the FUV flux is comparable for the two spirals:  $f_{H_\alpha}/f_{1521} = 14 \text{ \AA}$  for NGC 628, and  $10 \text{ \AA}$  for NGC 5457 (the units for  $f_{H_\alpha}$  are  $\text{ergs cm}^{-2} \text{ s}^{-1}$ , and for  $f_{1521}$  are  $\text{ergs cm}^{-2} \text{ s}^{-1} \text{ \AA}^{-1}$  — hence the units of  $\text{\AA}$  for the ratio of the fluxes). The average value of the ratio is

$$\frac{f_{H_\alpha}}{f_{1521}} \simeq 12 \text{ \AA}. \quad (17)$$

The observed  $H_\alpha$  flux from M31 is  $f_{H_\alpha} \simeq 5.1 \times 10^{-10} \text{ ergs cm}^{-2} \text{ s}^{-1}$  (Devereux et al. 1994). M31 is a highly inclined spiral with  $i = 77.5^\circ$  (Ma, Peng & Gu 1997). Adopting the average  $H_\alpha$  optical depth value  $\tau_{H_\alpha} = 1.23$  of Walterbos & Braun (1994) and assuming that the absorbing layer is thin, the deprojected face-on  $H_\alpha$  flux from M31 is  $\exp[\tau_{H_\alpha}(1 - \cos i)] \simeq 2.6$  times larger than the observed one, or  $f'_{H_\alpha} \simeq 1.3 \times 10^{-9} \text{ ergs cm}^{-2} \text{ s}^{-1}$ . Using the empirical conversion factor (equation [17]), we estimate the M31 face-on flux in B1 filter as  $f'_{1521} \simeq 1.1 \times 10^{-10} \text{ ergs cm}^{-2} \text{ s}^{-1} \text{ \AA}^{-1} \simeq 8.3 \text{ cm}^{-2} \text{ s}^{-1} \text{ \AA}^{-1}$ . We adopt the distance to M31 of 780 kpc (see discussion in Section 3.1). The FUV flux from M31 along its polar axis at the distance  $R_{\text{kpc}}$  expressed in units of the standard local FUV background with the flux  $F_{loc} = 2.0 \times 10^5 \text{ cm}^{-2} \text{ s}^{-1} \text{ \AA}^{-1}$  at  $\lambda = 1521 \text{ \AA}$  (Draine 1978) is then:

$$f_{ext} \simeq 25 R_{\text{kpc}}^{-2}. \quad (18)$$

Finally, dividing equation (16) by equation (18), we obtain a rough estimate of the ratio of the internal FUV flux to the flux from the host galaxy at the centre of the early-type dwarf satellites of M31 and the Milky Way (assuming, that the Milky Way FUV luminosity is comparable to that of M31):

$$\frac{f_{int}}{f_{ext}} \simeq 1.1 \times 10^{-6} I_0^{2/3} L_V^{1/3} R_{\text{kpc}}^2. \quad (19)$$

This equation is applicable to dwarfs located far from the plane of the host galaxy, where the dust attenuation becomes significant.

Using equation (19) and the data on dSphs from the

review of Mateo (1998), we can estimate the relative importance of the external FUV radiation for the Milky Way satellites. For all but one dSphs (Sextans, Ursa Minor, Draco, Carina, Sculptor, Fornax, and Leo II) the internal FUV flux is found to be much smaller than the external one even at the centre of the dwarf, with the  $f_{int}/f_{ext}$  values ranging from  $\sim 0.01$  (Sextans and Ursa Minor) to  $\sim 0.4$  (Fornax and Leo II). Leo I appears to be the only Galactic dSph for which the internal FUV flux at the centre of the dwarf dominates over the external one:  $f_{int}/f_{ext} \sim 2$ .

Equation (18) can also be used to determine whether the FUV flux from a large spiral galaxy is strong enough to affect the multi-phase structure of the ISM (and hence the star formation) in a nearby dwarf galaxy. Fig. 16 of Young & Lo (1997b) suggests that in low metallicity dwarf galaxies, FUV radiation, with the flux as low as 0.001 of the local Galactic value, can regulate the structure of the ISM. For M31 and the Milky Way, equation (18) indicates that the FUV flux will be larger than the above value out to a radius of 158 kpc, which encompasses most of the dwarf spheroidal satellites.

In an M31-like spiral, with low star formation activity and relatively small bulge, most of the FUV radiation comes from sources in the plane of the galaxy, closely associated with the spiral arms. The FUV flux from a normal spiral galaxy is then expected to be anisotropic, with most of the radiation near the plane of the galaxy being absorbed by the dust. In Fig. 9, we use two nearby spirals similar to M31 and the Milky Way, face-on NGC 5457 and edge-on NGC 891, to illustrate this anisotropy. A typical dSph galaxy on orbit around a giant spiral would spend most of its lifetime in the regime  $f_{int}/f_{ext} \ll 1$ , with relatively short periods of time of  $f_{int}/f_{ext} \gtrsim 1$  when the dwarf crosses the plane of the host spiral galaxy every 1 – 5 Gyr (half of the orbital period).

The above arguments appear to make a reasonably strong case for the external FUV radiation as being an important evolutionary factor for low mass dwarfs on orbits around large spirals.

There are two important caveats to the above analysis. The first one is related to the poorly known contribution from the metagalactic background to the FUV radiation field inside dwarf galaxies. The observed FUV background radiation is known to be strongly dominated by the local (Galactic) sources, making it almost impossible to put an accurate upper limit on the metagalactic flux (see discussion in Sasseen et al. 1995). Upper limits for the extragalactic background derived by different authors differ by more than an order of magnitude, and are as low as  $380 \text{ cm}^{-2} \text{ s}^{-1} \text{ \AA}^{-1}$  in  $4\pi$  solid angle at  $\lambda = 912 - 1100 \text{ \AA}$  (Murthy et al. 1999), or  $\sim 0.004$  in the local background units. Calculations of the propagation of FUV radiation from QSOs and AGNs through the intergalactic space (Haardt & Madau 1996, their fig. 5a) give an estimate of the lower limit for the background flux,  $28 \text{ cm}^{-2} \text{ s}^{-1} \text{ \AA}^{-1}$  at  $\lambda = 1000 \text{ \AA}$  ( $2.7 \times 10^{-4}$  in the local units). From equation (18), this range of possible background values corresponds to a radius  $83 < R < 310$  kpc for the sphere around M31 where its FUV radiation dominates over the background (except for the narrow zone near the plane of the galaxy).

The second caveat is that the heating by soft X-ray radiation, which is inferior to the FUV heating for the Galactic neutral ISM, could be the dominant heating mechanism

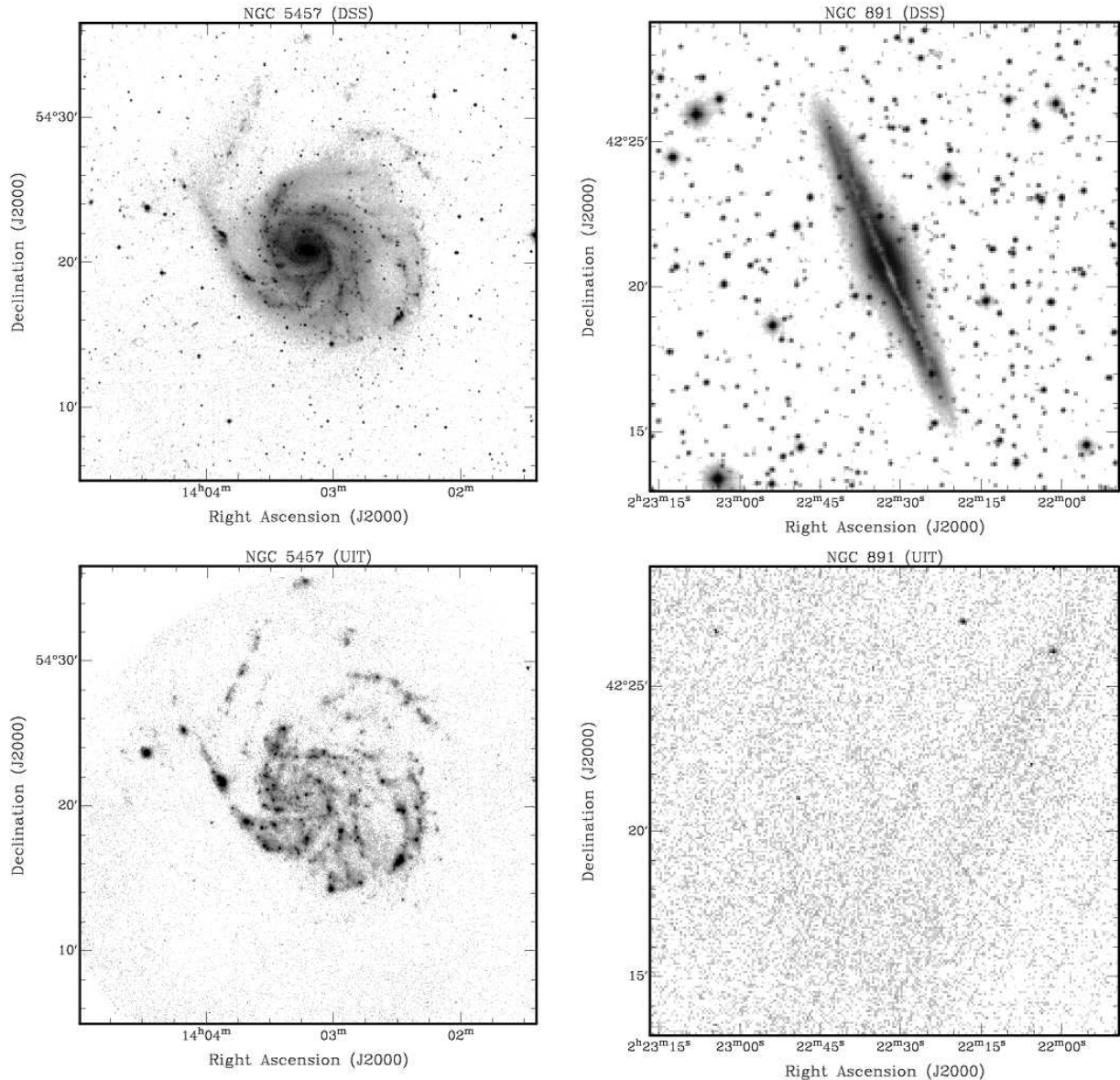


**Figure 9.** Optical DSS (top) and FUV UIT (bottom) images for two M31-like galaxies — face-on NGC 5457 (left panels), and edge-on NGC 891 (right panels). UIT images were obtained with B1 and B5 filters ( $\lambda \simeq 1500 \text{ \AA}$ ), and have comparable sensitivity (within a factor of 2). Weak features in both optical and FUV images were emphasized by using the square-root intensity scale. The fact that NGC 891 is not detected in FUV (bottom right image) points at the strong anisotropy of the FUV radiation field around normal spiral galaxies.

under the low metallicity and low radiation field conditions in dwarf galaxies (Wolfire et al. 1995). We estimate the M31 deprojected face-on X-ray luminosity in the band  $0.1 - 2 \text{ keV}$  to be  $\sim (0.5 - 1) \times 10^{40} \text{ ergs s}^{-1}$ . (For this we used the observed M31 soft X-ray luminosity value of  $0.43 \times 10^{40} \text{ ergs s}^{-1}$  from Supper et al. 2001, recalculated for the distance to M31 of 780 kpc, and the X-ray luminosity of the face-on spiral NGC 5457  $1.0 \times 10^{40} \text{ ergs s}^{-1}$  from Read & Ponman 2001, recalculated for the distance of 7.0 Mpc from Stetson et al. 1998.) The extragalactic soft X-ray background flux is believed to be known relatively accurately. Chen, Fabian & Gendreau (1997) give the following estimate of the background spectral density within the  $0.1 - 7 \text{ keV}$  band:  $10.5 E^{-1.46} \text{ keV cm}^{-2} \text{ s}^{-1} \text{ sr}^{-1} \text{ keV}^{-1}$ ,

where  $E$  is the photon energy in keV units. Integrated over the  $0.1 - 2 \text{ keV}$  interval of photon energies, this gives the following value for the metagalactic soft X-ray background flux (in  $2\pi$  solid angle):  $5.0 \times 10^{-7} \text{ ergs cm}^{-2} \text{ s}^{-1}$ . Combined with the derived above face-on X-ray luminosity of M31, the radius of the soft X-ray “dominance sphere” for M31 is found to be very small:  $\sim 9 - 13 \text{ kpc}$ . Thus the ISM heating by soft X-ray radiation from normal spiral galaxies cannot be an important environmental factor for dwarf galaxies.

This leads to the conclusion that FUV radiation escaping from spiral galaxies can be an important environmental factor for dwarf satellite galaxies only if the resultant ISM heating rate is larger than the heating rate from the metagalactic soft X-ray background. This issue can be addressed

only through solving numerically the equations of thermal and ionization equilibrium with the inclusion of all the relevant physical processes (similarly to Wolfire et al. 1995), which is beyond the scope of this paper.

### 3 OBSERVATIONAL EVIDENCE

The previous section gives support to the idea that the electromagnetic radiation escaping from the host spiral galaxy can be an important evolutionary factor for dwarf galaxies. This mechanism can explain in general the principal differences (in SFHs and neutral gas content) between two classes of dwarfs — dSphs and dIrrs. In this section we will present observational evidences for the impact of the UV radiation from the Milky Way and M31 on their dwarf satellites, which gives further support to the above idea.

#### 3.1 The puzzle of the “twin” galaxies NGC 147 and NGC 185

The two dwarf elliptical satellites of M31, NGC 147 and NGC 185, appear to be almost identical in many respects (Young & Lo 1997a): they have comparable blue luminosities, Holmberg diameters,  $B-V$  colors, average surface brightness, light profile shapes, mean stellar dispersions, and projected distances from M31. Both galaxies show evidence for an intermediate-age stellar component (Young & Lo 1997a).

Despite all these similarities, NGC 147 and NGC 185 are strikingly different in their recent SFHs, and in the present day neutral gas content. NGC 185 formed stars as recently as 20 Myr ago (Lee et al. 1993a), and contains substantial amounts of H I ( $1.1 \times 10^5 M_{\odot}$ ) and H<sub>2</sub> ( $4.1 \times 10^4 M_{\odot}$ ) (Young 2001). Conversely, NGC 147 has not formed stars for at least a Gyr (Han et al. 1997), and appears to be devoid of neutral ISM (Young & Lo 1997a; Sage, Welch & Mitchell 1998).

We argue that the differences between NGC 147 and NGC 185 can be explained by different fluxes of the LyC and FUV radiation escaping from M31 at the present locations of the dwarfs.

To quantify this effect, we need to know the accurate distances to the dwarfs and to M31. To avoid large systematic errors, we use the distance measurements obtained with the same technique — the tip of the red giant branch (TRGB) method, which was shown to work very well for low-metallicity Population II stars (Lee, Freedman & Madore 1993b). Two available TRGB distance measurements for NGC 185 (Lee et al. 1993b and Martínez-Delgado & Aparicio 1998) give virtually the same values of the true distance modulus:  $(m - M)_0 = 23.95 \pm 0.1$ . The situation with NGC 147 is different — Lee et al. (1993b) gave the value  $(m - M)_0 = 24.13 \pm 0.1$ , whereas Han et al. (1997) obtained  $(m - M)_0 = 24.37 \pm 0.06$ . We choose to use the latter value, because it was derived from the high quality WFCP2 data for  $\sim 117,000$  stars in two different fields, both producing identical true distance modulus estimates. In contrast, the distance value of Lee et al. (1993b) was based on the photometry of only  $\sim 500$  stars from the paper of Mould, Kristian & Da Costa (1983). Two relevant distance measurements for M31 agree very well:

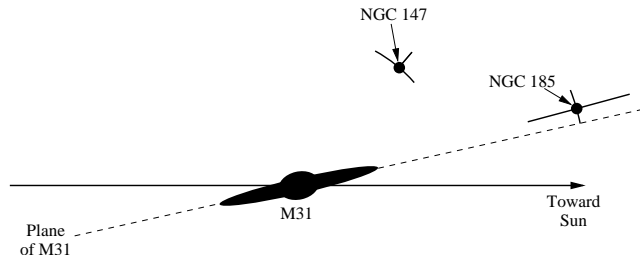


**Figure 10.** The most probable locations of NGC 147 and NGC 185 relative to the disk of M31 and the observer. The error bars correspond to one-sigma confidence intervals. Please note that the disk of M31 is not drawn to scale.

Durrell, Harris & Pritchett (2001) obtained a TRGB true distance modulus  $(m - M)_0 = 24.47 \pm 0.12$  based on wide-field photometry of a field in the outer halo of M31, and Holland (1998) derived  $(m - M)_0 = 24.47 \pm 0.07$  by fitting theoretical isochrones to the observed red giant branches of 14 globular clusters in M31. (It is interesting to note that an identical value was also obtained by Stanek & Garnavich (1998) from comparing the red clump stars with parallaxes known to better than 10% in the Hipparcos catalog with the red clump stars observed in three fields in M31 using the Hubble Space Telescope:  $(m - M)_0 = 24.47 \pm 0.08$ .) Finally, we adopt the following values of the true distance modulus for NGC 185, NGC 147, and M31:  $23.95 \pm 0.1$ ,  $24.37 \pm 0.06$ , and  $24.47 \pm 0.07$ , respectively.

We derive the following distances from M31:  $100^{+13}_{-4}$  kpc for NGC 147, and  $186^{+34}_{-33}$  kpc for NGC 185. If the FUV and ionizing radiation from M31 were isotropic, NGC 147 would receive  $2.8^{+0.9}_{-0.8}$  times larger flux than NGC 185. This difference is probably not large enough to explain the observed differences in the neutral gas content and recent SFH of the dwarfs.

It is expected though that the LyC and FUV fluxes from a giant spiral galaxy are strongly anisotropic, being at maximum along the polar axis (local galactic latitude  $b_{loc} = \pm 90^\circ$ ), and dropping virtually to zero in the plane of the galaxy ( $b_{loc} = 0^\circ$ ). To estimate  $b_{loc}$  values for NGC 147 and NGC 185, we adopt the inclination angle of the M31 disk  $i = 77^\circ.5$  from Ma et al. (1997), and the position angle of the galactic line of nodes  $PA = 37^\circ.7$  from de Vaucouleurs (1958). The uncertainty in both angles is assumed to be  $1^\circ$ . We use the fact that the northwest side of M31 is the near side (e.g. Walterbos & Kennicutt 1988), and arbitrarily choose the local northern pole to be on the opposite side of the M31 disk.

Taking into account all the uncertainties, we derive  $b_{loc} = (3^{+4}_{-3})$  dgr. for NGC 185, and  $b_{loc} = (37^{+11}_{-8})$  dgr. for NGC 147. It appears that NGC 185 is located almost in the plane of the M31 disk, and is therefore shielded from the FUV and LyC electromagnetic radiation by the H I disk of M31. In contrast, from the location of NGC 147 the M31 spiral is seen half-open (see Fig. 10), resulting in significant fluxes of the ionizing and FUV radiation, which can ionize and heat the ISM of the dwarf, thus preventing star formation.

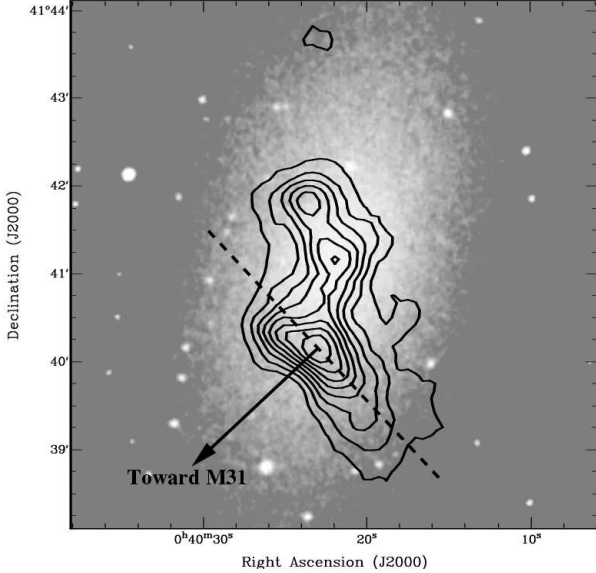


**Figure 11.** H I flux contours of NGC 205 from Young & Lo (1997a), superposed on a DSS image (only the central brightest part of the optical disk is shown). The arrow shows the direction toward the M31 centre at PA = 133°. The dashed line is perpendicular to the arrow.

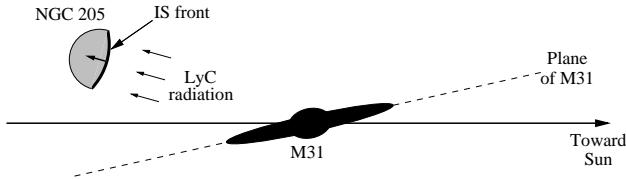


**Figure 12.** Scheme showing a probable position of NGC 205 relative to M31 and the observer. In this configuration the IS front in the ISM of NGC 205 would be seen by the observer red-shifted relative to the stars of the dwarf galaxy. Please note that the bodies of M31 and NGC 205 are not drawn to scale.

### 3.2 Disturbed ISM of NGC 205

The neutral ISM of the NGC 205 dwarf elliptical satellite of M31 consists of  $4.3 \times 10^5 M_{\odot}$  of H I and  $\sim 1 \times 10^5 M_{\odot}$  of H<sub>2</sub> (Young 2000). The morphology and kinematics of the neutral gas is very unusual: the central and northern parts of the ISM look relatively unperturbed with the radial velocity being close to that of the stellar body, whereas the southern part appears to be compressed in the SE direction and red-shifted by  $\sim 20 - 30 \text{ km s}^{-1}$  relative to the stars (Young & Lo 1997a, their fig. 2 and 4).

We note that the line drawn along the compressed gas in the southern part of the galaxy is perpendicular to the direction toward the centre of M31, which is located to the south-east of NGC 205 at the position angle PA = 133° (Fig. 11). The dwarf galaxy is located very close to M31 in projection (8 kpc away at the distance of M31), and most probably is  $\sim 30 - 100 \text{ kpc}$  behind the spiral galaxy along the line of sight (Saha et al. 1992; Mateo 1998; Bond & Alves 2001). This places NGC 205 relatively close to the plane of the spiral galaxy, with the local galactic latitude  $b_{loc} \sim 20^{\circ}$ . The morphology and kinematics of the disturbed gas is then consistent with an ionization-shock (IS) front driven by the LyC

radiation from M31 toward the centre of NGC 205 with a velocity of  $\sim 25 \text{ km s}^{-1}$  (Fig. 12). The fact that the compressed part of the ISM shows the highest H I column density in NGC 205 and contains significant amounts of H<sub>2</sub> kinematically coupled to the H I (Young 2000) supports this picture of a relatively strong shock. From Fig. 11, we estimate that the shock front has already traveled  $\sim 300 \text{ pc}$  inside the dwarf, indicating that the process started very recently:  $\sim 10 \text{ Myr}$  ago (kinematic age).

Another important piece of evidence comes from the SFH of the dwarf galaxy. The central part of NGC 205 has experienced two recent star bursts — 20–80 and  $\sim 500 \text{ Myr}$  ago, with a puzzling gap in between (Lee 1996).

We propose the following scenario which explains both the ISM and the recent SFH peculiarities of NGC 205. We argue that the dwarf galaxy experienced the two most recent star bursts during its passages through the plane of M31. The star formation 20–80 Myr ago, the dwarf’s present location close to the plane of the spiral, and the short time scale  $\sim 10 \text{ Myr}$  for the observed IS front all suggest that NGC 205 has recently crossed the plane of M31. Associating the second to last star burst  $\sim 500 \text{ Myr}$  ago with the previous crossing of the plane gives an estimate of the orbital period of the dwarf:  $P \simeq 1 \text{ Gyr}$ . If we assume that the dwarf is on circular orbit around M31 with the orbital velocity  $V_c = 220 \text{ km s}^{-1}$ , then the radius of the orbit is 36 kpc. At such a small distance, the LyC and FUV fluxes from M31 should be significant for most of the lifetime of NGC 205, with only short periods every 500 Myr with much lower levels of radiation during the passages through the plane of the host spiral galaxy.

### 3.3 Carina dSph versus Ursa Minor dSph

Carina and Ursa Minor dwarf spheroidals belong to the class of the lowest luminosity dSph galaxies. They have comparable luminosity ( $L_V \sim [3 - 4] \times 10^5 L_{\odot}$ ), core radius ( $r_c \sim 200 \text{ pc}$ ), central mass-to-light ratio ( $m/L_V \sim 30 - 60$ ), and distance from the Milky Way galaxy ( $R \sim 70 - 100 \text{ kpc}$ ) (Mateo 1998). It is very surprising then that they exhibit two opposite SFH extremes: Carina has formed stars for most of its lifetime in three discrete bursts 3, 7, and 15 Gyr ago (Hurley-Keller et al. 1998), whereas Ursa Minor was formed in a single star burst  $\gtrsim 14 \text{ Gyr}$  ago (Olszewski & Aaronson 1985; Hernandez, Gilmore & Valls-Gabaud 2000).

We note that Carina has the smallest absolute value of the galactic latitude  $\|b\| \simeq 22^{\circ}$  among all the Milky Way satellite galaxies (excluding the special case of the Sagittarius dSph). This is consistent with Carina having relatively small angle between its orbit and the plane of the Galaxy — probably as small as  $22^{\circ}$ . If this is the case, the dwarf has spent a significant part of its lifetime hiding from the ionizing and FUV radiation from the Milky Way near the plane of the Galaxy, keeping its ISM neutral and episodically forming stars.

The opposite example is that of Ursa Minor. Both the proper motion measurements (Schweitzer et al. 1997) and the relatively high location above the Galactic plane ( $\|b\| \simeq 45^{\circ}$ ) suggest that the dwarf is on a close to polar orbit around the Milky Way galaxy. Galaxies less massive than  $\sim 2 \times 10^8 M_{\odot}$  should gradually lose their ISM when the gas is fully photoionized. We argue that the relatively small

distance from the Galaxy and the almost polar orbit caused Ursa Minor to lose its ISM on a short time scale, leading to sharply declining SFR.

#### 4 DISCUSSION AND CONCLUSIONS

Theoretical description of the formation and evolution of dwarf irregular galaxies is a complex problem, which is far from being fully resolved. Nevertheless, recent semi-analytical models (Spaans & Norman 1997; Ferrara & Tolstoy 2000) appear to converge in that the isolated gas-rich dwarfs should have been forming stars with almost constant low efficiency for most of their lifetimes, with a possible exception of the early epoch ( $z \gtrsim 1$ ) with increased SFR. The emerging consensus is that soon after the initial star burst, the star formation becomes self-regulated through the feedback from massive stars (impact on the ISM of stellar winds, ionizing and FUV radiation, and supernovae). This is in accord with the findings of van Zee (2001), who showed that observed optical colors of a large sample of isolated dIrr galaxies are consistent with approximately constant SFR for at least 10 Gyr.

The situation with early-type dwarfs (dSph and dE) is even more complicated. There are at least three observational facts that any successful dwarf evolution theory should explain:

(i) *Impact of environment.* All Local Group dwarfs with  $M_V > -15^m$  located within 250 kpc from Milky Way and M31 are early-type systems. The observed morphology-density relation for dwarf galaxies (Binggeli, Tarengi & Sandage 1990) appears to extend this trend beyond the Local Group.

(ii) *Absence of neutral gas.* With a few exceptions, the Local Group early-type dwarfs appear to be devoid of H I and H<sub>2</sub> — despite showing in many cases the evidence for recent star formation. For example, Fornax has a very low H I mass upper limit of 5,000  $M_\odot$  (Mateo 1998), but formed stars as recently as 200 Myr ago (Saviane, Held & Bertelli 2000).

(iii) *Episodic SFH.* Some Local Group dSph/dE galaxies have puzzling gaps of 1 – 5 Gyr in their SFHs. These time intervals are much longer than the  $10^7 - 10^8$  yr timescales of internal mechanisms which could effect the star formation, — with a possible exception of the SNe Ia heating mechanism (Burkert & Ruiz-Lapuente 1997).

In this paper we showed that all the above observational facts can be explained by the impact of the ultraviolet radiation from the host spiral galaxy on the ISM of dwarf satellites. We gave evidence in support of the following key ingredients of our model:

(i) FUV and LyC fluxes from giant spiral galaxies are sufficiently large to alter the state of the ISM in nearby dwarf galaxies such that star formation becomes unlikely. The LyC radiation can ionize the ISM through the process of photoevaporation, making it very hard to detect.

(ii) The UV radiation from spiral galaxies like the Milky Way and M31 dominates over the metagalactic background radiation within a large sphere of radius  $\sim 200$  kpc.

(iii) The ultraviolet radiation field of a spiral galaxy is

strongly anisotropic, with the flux dropping almost to zero in the narrow zone near the plane of the galaxy.

In our scenario, low mass galaxies orbiting around large spirals spend most of their lifetimes exposed to the ultraviolet radiation from their host galaxies, which keeps their ISM in warm ( $\sim 10^4$  K) and ionized state. Twice per orbital period, each satellite crosses a narrow “shadow” zone near the plane of host galaxy, where the ultraviolet flux is dramatically reduced by the absorption in the H I disk of the spiral. During such “eclipses”, the ISM of the dwarf galaxy can recombine, cool down, and collapse toward the centre of the dwarf on timescales of  $\sim 100$  Myr. We expect the cold dense gas at the centre of the dwarf to become self-gravitating, and under favorable conditions to start forming stars. For a short time, such early-type dwarfs can turn into a dIrr galaxy, with the two-phase ISM structure, and the low efficiency star formation self-regulated through the feedback mechanisms. Approaching the edge of the shadow zone, the dwarf galaxy experiences an increase in the external FUV flux, which can warm up the ISM and quench the star formation. Finally, the increased LyC flux can photoionize the warm ISM through the process of photoevaporation.

An important issue we have to address is whether observations of high-velocity clouds (HVCs) are consistent with our scenario. HVCs are H I clouds which are well separated in radial velocity from the Galactic H I disk (Wakker & van Woerden 1991). With a few exceptions, distances to HVCs are either unknown or strongly model-dependent (like Magellanic Stream). The range of plausible distances is from a few kpcs to hundreds of kpcs. Many HVCs were detected in H $\alpha$  emission line (Putman et al. 2003). Typical H $\alpha$  emission measures range from  $\sim 30$  to  $\sim 600$  mR, which would correspond to the distances of 14–67 kpc in our simplified description of the Galactic ionizing radiation field. Two Sculptor H I clouds (Carignan et al. 1998), that are most probably physically associated with the Sculptor dSph (Bouchard et al. 2003), would have a low peak H $\alpha$  flux of 22 mR in our Galactic LyC model, which is consistent with a  $< 26$  mR nondetection of Putman et al. (2003). Among different hypotheses on the origin of HVCs, our radiation harassment model is consistent with those that place these clouds in the Galactic halo at distances  $> 15$  kpc from the Galactic centre. The possible scenarios include accretion of warm-hot intergalactic medium, stripped gas from disrupted Galactic satellites, and gas-rich DM-dominated subhalos. Recent detection of HVCs around M31 galaxy (Thilker et al. 2004) appears to be consistent with the above scenarios.

One of predictions of our model which can be tested observationally is that at least some early-type dwarf satellites of the Milky Way and M31 should possess extended ionized ISM, with the temperature  $T \sim 10^4$  K, and low number density. The total mass of the gas can be comparable to the mass of the stars. The sound speed in the photoionized gas ( $\sim 10$  km s $^{-1}$ ) is close to the stellar velocity dispersion in dSphs, hence both gas and stars are expected to have a comparable extent (see also Fig. 8). The most promising candidates are the dwarfs with complex and relatively recent star formation, located  $\lesssim 100$  kpc away from the host galaxy: NGC 147, Fornax, and Carina.

There are two possible ways to detect such tenuous ion-

ized gas: either in absorption, by obtaining FUV spectra of QSOs and AGNs located behind the dwarf, or through its emission (e.g., in  $H_\alpha$  line).

The absorption method was used by Bowen et al. (1997), who put an upper limit on the column density of the ionized gas around Leo I. They probed with HST three sight lines toward QSOs passing  $\geq 34'$  from the centre of the dwarf, and did not detect any absorption in C IV, Si II, or Si IV spectral lines at the velocity of Leo I. The photoionized gas in this dwarf (if present) is not expected to extend far beyond its stellar tidal radius, which is equal to 12.6 (Mateo 1998), so the results of Bowen et al. (1997) cannot be used to test our model. Bowen et al. also showed, that with the present day technology only the brightest quasars, with  $m_V \lesssim 16^m$ , can be used to search for the presence of the tenuous ionized gas in dSphs. To the best of our knowledge, there are no known QSO/AGN, brighter than  $m_V \sim 17^m$ , located in projection within the stellar extent of the Local Group early-type dwarfs (Tinney, Da Costa & Zinnecker 1997; Tinney 1999; Schneider et al. 2002).

We believe that the ionized ISM detection in  $H_\alpha$  emission line is a more feasible approach. The expected  $H_\alpha$  surface brightness is  $< 100$  mR, so the required sensitivity of the observations should be at least 10 mR. The angular resolution should be at least  $\sim 10'$  for the Milky Way satellites, and  $\sim 1'$  for the M31 companions. The Galactic foreground radiation is expected to dominate over the radiation coming from the dwarfs (with the typical integral flux values of  $\sim 1$  R for the high Galactic latitude dwarfs, and reaching  $\sim 20$  R for Carina), so the observations should be carried out within a narrow, 20–40  $\text{km s}^{-1}$ , interval of the radial velocities centred at the optical velocity of the dwarf. Three available wide-field  $H_\alpha$  surveys do not meet the above requirements: two complementing surveys, VTSS<sup>1</sup> (Virginia Tech Spectral-Line Survey, covers northern hemisphere, Dennison, Simonetti & Topasna 1998), and SHASSA<sup>2</sup> (Southern H-Alpha Sky Survey Atlas, Gaustad et al. 2001) lack sensitivity (500 mR) and velocity information, whereas WHAM<sup>3</sup> (covers northern hemisphere, Reynolds et al. 1998) having reasonably good sensitivity (50 mR) and spectral resolution ( $\sim 10$   $\text{km s}^{-1}$ ), does not qualify because of the insufficient angular resolution ( $1^\circ$ ) and too narrow velocity coverage:  $V_{\text{LSR}} = -100 \dots 100$   $\text{km s}^{-1}$ . Targeted  $H_\alpha$  emission observations can do a much better job: observations with the sensitivity  $\sim 10$  mR, angular and velocity resolutions  $\sim 5'$  and  $\sim 10$   $\text{km s}^{-1}$ , are almost routine nowadays (Weiner et al. 2002; Weymann et al. 2001). With new differential techniques, even lower emission levels of 1–2 mR might be reached (Bland-Hawthorn & Maloney 2001).

It is interesting to note, that at least one of the dwarf galaxies in question, NGC 205, has a tentative extended  $H_\alpha$  emission detection in VTSS<sup>4</sup> (field And07). The central part of the dwarf has a surface brightness of  $\sim 5$  R, and the fainter emission with the brightness of 1–2 R appears to fill out all the stellar extent of the galaxy. These large values of the

$H_\alpha$  flux, if confirmed, might require alternative explanations as to the source of ionization. Future targeted  $H_\alpha$  emission observations of NGC 205 are required to resolve the issue.

## ACKNOWLEDGMENTS

We are grateful to Frank Bertoldi, Andrea Ferrara, and Sergey Silich for insightful discussions and numerous helpful suggestions. We also thank Lisa Young for providing the H I data for NGC 205. C. C. acknowledges support from NSERC (Canada) and FCAR (Québec).

## REFERENCES

- Barnes D. G., de Blok W. J. G., 2001, *AJ*, 122, 825  
 Bell E. F., Kennicutt R. C., 2001, *ApJ*, 548, 681  
 Bertoldi F., 1989, *ApJ*, 346, 735  
 Bertoldi F., McKee C. F., 1990, *ApJ*, 354, 529  
 Bianchi S., Cristiani S., Kim T.-S., 2001, *A&A*, 376, 1  
 Binggeli B., Tarenghi M., Sandage A., 1990, *A&A*, 228, 42  
 Binney J., Tremaine S., 1994, *Galactic Dynamics* (3d ed.). Princeton Univ. Press, Princeton, NJ  
 Bland-Hawthorn J., Maloney P. R., 2001, in Mulchaey J. S., Stocke J., eds, *ASP Conf. Ser. Vol. 254, Extragalactic Gas at Low Redshift*. Astron. Soc. Pac., San Francisco, p. 267  
 Bond H. E., Alves D. R., 2001, in Szczerba R., Gorny S. K., eds, *Astrophysics and Space Science Library Vol. 265, Post-AGB Objects as a Phase of Stellar Evolution*. Kluwer Academic Publishers, Boston/Dordrecht/London, p. 77  
 Bouchard A., Carignan C., Mashchenko S., 2003, *AJ*, 126, 1295  
 Bowen D. V., Tolstoy E., Ferrara A., Blades J. C., Brinks E., 1997, *ApJ*, 478, 530  
 Burkert A., 1995, *ApJ*, 447, L25  
 Burkert A., Ruiz-Lapuente P., 1997, *ApJ*, 480, 297  
 Carignan C., Beaulieu S., Côté S., Demers S., Mateo M., 1998, *AJ*, 116, 1690  
 Chen L.-W., Fabian A. C., Gendreau K. C., 1997, *MNRAS*, 285, 449  
 de Vaucouleurs G., 1958, *ApJ*, 128, 465  
 Dennison B., Simonetti J. H., Topasna G. A., 1998, *Publications of the Astronomical Society of Australia*, 15, 147  
 Devereux N. A., Price R., Wells L. A., Duric N., 1994, *AJ*, 108, 1667  
 Draine B. T., 1978, *ApJS*, 36, 595  
 Durrell P. R., Harris W. E., Pritchett C. J., 2001, *AJ*, 121, 2557  
 Ferrara A., Tolstoy E., 2000, *MNRAS*, 313, 291  
 Gallagher J. S., Madsen G. J., Reynolds R. J., Grebel E. K., Smecker-Hane T. A., 2003, *ApJ*, 588, 326  
 Gallart C., Martínez-Delgado D., Gómez-Flechoso M. A., Mateo M., 2001, *AJ*, 121, 2572  
 Gaustad J. E., McCullough P. R., Rosing W., Van Buren D., 2001, *PASP*, 113, 1326  
 Grebel E. K., 1997, *Reviews of Modern Astronomy*, 10, 29  
 Haardt F., Madau P., 1996, *ApJ*, 461, 20  
 Han M., Hoessel J. G., Gallagher J. S., Holtzman J., Stetson P. B., 1997, *AJ*, 113, 1001

<sup>1</sup> <http://www.phys.vt.edu/~halph>

<sup>2</sup> <http://amundsen.swarthmore.edu/SHASSA>

<sup>3</sup> <http://www.astro.wisc.edu/wham>

<sup>4</sup> The Virginia Tech Spectral-Line Survey (VTSS) is supported by the National Science Foundation.

- Hayashi E., Navarro J. F., Taylor J. E., Stadel J., Quinn T., 2003, *ApJ*, 584, 541
- Hernandez X., Gilmore G., Valls-Gabaud D., 2000, *MNRAS*, 317, 831
- Holland S., 1998, *AJ*, 115, 1916
- Hurley-Keller D., Mateo M., Nemeč J., 1998, *AJ*, 115, 1840
- Johnston K. V., 1998, *ApJ*, 495, 297
- Lee M. G., Freedman W. L., Madore B. F., 1993a, *AJ*, 106, 964
- Lee M. G., Freedman W. L., Madore B. F., 1993b, *ApJ*, 417, 553
- Lee M. G., 1996, *AJ*, 112, 1438
- Lefloch B., Lazareff B., 1994, *A&A*, 289, 559
- Lokas E. L., 2002, *MNRAS*, 333, 697
- Ma J., Peng Q., Gu Q., 1997, *ApJ*, 490, L51
- Martínez-Delgado D., Aparicio A., 1998, *AJ*, 115, 1462
- Martínez-Delgado D., Gallart C., Aparicio A., 1999, *AJ*, 118, 862
- Mateo M. L., 1998, *ARA&A*, 36, 435
- Mayer L., Governato F., Colpi M., Moore B., Quinn T., Wadsley J., Stadel J., Lake G., 2001, *ApJ*, 559, 754
- Miller B. W., Dolphin A. E., Lee M. G., Kim S. C., Hodge P., 2001, *ApJ*, 562, 713
- Mould J. R., Kristian J., Da Costa G. S., 1983, *ApJ*, 270, 471
- Murthy J., Hall D., Earl M., Henry R. C., Holberg J. B., 1999, *ApJ*, 522, 904
- Odenkirchen M. et al., 2001, *AJ*, 122, 2538
- Olszewski E. W., Aaronson, M., 1985, *AJ*, 90, 2221
- Piatek S. et al., 2002, *AJ*, 124, 3198
- Piersimoni A. M., Bono G., Castellani M., Marconi G., Cassisi S., Buonanno R., Nonino M., 1999, *A&A*, 352, L63
- Putman M. E., Bland-Hawthorn J., Veilleux S., Gibson B. K., Freeman K. C., Maloney P. R., 2003, *ApJ*, 597, 948
- Read A. M., Ponman, T. J., 2001, *MNRAS*, 328, 127
- Reynolds R. J., Tufte S. L., Haffner L. M., Jaehnig K., Percival J. W., 1998, *Publications of the Astronomical Society of Australia*, 15, 14
- Sage L. J., Welch G. A., Mitchell G. F., 1998, *ApJ*, 507, 726
- Saha A., Hoessel J. G., Krist J., 1992, *AJ*, 103, 84
- Sassee, T. P., Lampton, M., Bowyer, S., Wu, X., 1995, *ApJ*, 447, 630
- Saviane I., Held E. V., Bertelli G., 2000, *A&A*, 355, 56
- Schneider D. P. et al., 2002, *AJ*, 123, 567
- Schweitzer A. E., Cudworth K. M., Majewski S. R., 1997, in Humphreys R. M., ed., *ASP Conf. Ser. Vol. 127, Proper Motions and Galactic Astronomy*. Astron. Soc. Pac., San Francisco, p. 103
- Shull J. M., Roberts D., Giroux M. L., Penton S. V., Fardal M. A., 1999, *AJ*, 118, 1450
- Silk J., Wyse R. F. G., Shields G. A., 1987, *ApJ*, 322, L59
- Spaans M., Norman, C. A., 1997, *ApJ*, 483, 87
- Spitzer L., Jr., 1978, *Physical Processes in the Interstellar Medium*. Wiley-Interscience, New York
- St-Germain J., Carignan C., Côte S., Oosterloo T., 1999, *AJ*, 118, 1235
- Stanek K. Z., Garnavich P. M., 1998, *ApJ*, 503, L131
- Stecher T. P. et al., 1997, *PASP*, 109, 584
- Sternberg A., McKee C. F., Wolfire M. G., 2002, *ApJS*, 143, 419
- Stetson P. B. et al., 1998, *ApJ*, 508, 491
- Stoehr F., White S. D. M., Tormen G., Springel V., 2002, *MNRAS*, 335, L84
- Supper R., Hasinger G., Lewin W. H. G., Magnier E. A., van Paradijs J., Pietsch W., Read A. M., Trümper J., 2001, *A&A*, 373, 63
- Sutherland R. S., Dopita M. A., 1993, *ApJS*, 88, 253
- Thilker D. A., Braun R., Walterbos R. A. M., Corbelli E., Lockman F. J., Murphy E., Maddalena R., 2004, *ApJ*, 601, L39
- Tinney C. G., Da Costa G. S., Zinnecker H., 1997, *MNRAS*, 285, 111
- Tinney C. G., 1999, *MNRAS*, 303, 565
- van den Bergh S., 1999, *AJ*, 117, 2211
- van Zee L., 2001, *AJ*, 121, 2003
- Wakker B. P., van Woerden H., 1991, *A&A*, 250, 509
- Walterbos R. A. M., Braun R., 1994, *ApJ*, 431, 156
- Walterbos R. A. M., Kennicutt R. C., 1988, *A&A*, 198, 61
- Weiner B. J., Vogel S. N., Williams T. B., 2002, in Mulchaey J. S., Stocke J., eds, *ASP Conf. Ser. Vol. 254, Extragalactic Gas at Low Redshift*. Astron. Soc. Pac., San Francisco, p. 256
- Welch G. A., Mitchell G. F., Yi S., 1996, *ApJ*, 470, 781
- Weymann R. J., Vogel S. N., Veilleux S., Epps H. W., 2001, *ApJ*, 561, 559
- Wolfire M. G., Hollenbach D., McKee C. F., Tielens A. G. G. M., Bakes E. L. O., 1995, *ApJ*, 443, 152
- Young L. M., Lo K. Y., 1996, *ApJ*, 462, 203
- Young L. M., Lo K. Y., 1997a, *ApJ*, 476, 127
- Young L. M., Lo K. Y., 1997b, *ApJ*, 490, 710
- Young L. M., 2000, *AJ*, 120, 2460
- Young L. M., 2001, *AJ*, 122, 1747